Basolateral Na^+-H^+ Antiporter

Mechanisms of Electroneutral and Conductive Ion Transport

MARC A. POST and DAVID C. DAWSON

From the Department of Physiology, University of Michigan Medical School, Ann Arbor, Michigan 48109-0622

ABSTRACT The basolateral Na-H antiporter of the turtle colon exhibits both conductive and electroneutral Na^+ transport (Post and Dawson. 1992. *American Journal of Physiology*. 262:C1089–C1094). To explore the mechanism of antiporter-mediated current flow, we compared the conditions necessary to evoke conduction and exchange, and determined the kinetics of activation for both processes. Outward (cell to extracellular fluid) but not inward (extracellular fluid to cell) Na^+ or Li^+ gradients promoted antiporter-mediated Na^+ or Li^+ currents, whereas an outwardly directed proton gradient drove inward Na^+ or Li^+ currents. Proton gradient–driven, "counterflow" current is strong evidence for an exchange stoichiometry of > 1 Na^+ or Li^+ per proton. Consistent with this notion, outward Na^+ and Li^+ currents generated by outward Na^+ or Li^+ gradients displayed sigmoidal activation kinetics. Antiporter-mediated proton currents were never observed, suggesting that only a single proton was transported per turnover of the antiporter. In contrast to Na^+ conduction, Na^+ exchange was driven by either outwardly or inwardly directed Na^+, Li^+, or H^+ gradients, and the activation of Na^+/Na^+ exchange was consistent with Michaelis-Menten kinetics ($K_{1/2} = 5$ mM). Raising the extracellular fluid Na^+ or Li^+ concentration, but not extracellular fluid proton concentration, inhibited antiporter-mediated conduction and activated Na^+ exchange. These results are consistent with a model for the Na-H antiporter in which the binding of Na^+ or Li^+ to a high-affinity site gives rise to one-for-one cation exchange, but the binding of Na^+ or Li^+ ions to other, lower-affinity sites can give rise to a nonunity, cation exchange stoichiometry and, hence, the net translocation of charge. The relative proportion of conductive and nonconductive events is determined by the magnitude and orientation of the substrate gradient and by the serosal concentration of Na^+ or Li^+.

Address correspondence to Dr. David C. Dawson, Department of Physiology, University of Michigan, Ann Arbor, MI 48109-0622.

Dr. Post's present address is Division of Molecular Medicine and Genetics, Department of Internal Medicine, University of Michigan Medical Center, 4570 MSRB II, Box 0650, University of Michigan, Ann Arbor, MI 48109-0650.

J. GEN. PHYSIOL. © The Rockefeller University Press · 0022-1295/94/05/0895/22 $2.00
Volume 103 May 1994 895–916

INTRODUCTION

We recently characterized a volume-sensitive, basolateral Na-H antiporter that exhibited both electroneutral Na^+ exchange and a Na^+ conductance (Post and Dawson, 1992). The antiporter was active in shrunken but not swollen cells; was blocked by ethylisopropylamiloride (EIPA) (K_i = 350 nM), dimethylamiloride (DMA) (K_i = 700 nM), and amiloride (K_i = 10 μM); catalyzed Na/H, Na/Na, and Na/Li exchange; and mediated outward (i.e., cell to extracellular fluid [ecf]), but not inward (i.e., ecf to cell), Na^+ or Li^+ currents. At least two other transporters are known to exhibit both electroneutral and conductive operating modes: the Na,K-ATPase (Kaplan, Durham, Logue, and Kenney, 1984) and the Cl/HCO_3 exchanger (Kaplan, Pring, and Passow, 1983; Knauf, Law, and Merchant, 1983). The conductive operating mode of the Na,K-ATPase has been relatively well characterized, in part because the perfused squid axon (De Weer and Rakowski, 1984) and internally dialyzed cardiac myocytes (Gadsby, Nakao, Bahinski, Nagel, and Suenson, 1992) provide access to both the intracellular and extracellular faces of the transporter in cells that express high levels of Na/K pump activity. Cl^- conduction by the Cl/HCO_3 exchanger has not been studied electrophysiologically, but has been inferred from valinomycin induced net KCl efflux from erythrocytes (Hunter, 1977). The goal of the studies described here was to investigate the mechanism of antiporter-mediated cation conduction. The apically permeabilized colonic cell layer employed in this study provided the opportunity to study the steady state kinetics of conductive transport and compare them with those of cation exchange. We characterized the activation kinetics, cation selectivities, and inhibitor specificities of electroneutral exchange and cation conduction and investigated the conditions required to generate either outward or inward antiporter-mediated currents. These data are interpreted in terms of a mechanistic model of the Na/H antiporter that could have implications for future studies aimed at determining the relationship between protein structure and antiporter function.

Models for Conductive Ion Flow

A generic model for electroneutral Na-H antiport, adapted from Stein (1986) and Fröhlich and Gunn (1986), is diagrammed in Fig. 1 *A*. The model is derived from the notion of a "ping-pong" catalytic cycle for the antiporter, i.e., a single cation binding site that is alternately exposed to the compartments on either side of the membrane so that one cation is bound, translocated, and released before the binding of another cation. In the diagram, X_o denotes the outward-facing conformation of the antiporter protein and X_i denotes the inward-facing conformation. The model in Fig. 1 *A* is constrained by the condition that in order for the transition between the inward- and outward-facing conformations to occur the binding site must be occupied (i.e., the transitions $X_iNa \rightleftarrows X_oNa$ and $X_iH \rightleftarrows X_oH$ are allowed whereas the transition $X_i \rightleftarrows X_o$ is not). One general consequence of this constraint is that cation gradients will determine the time average probability that the empty antiporter will reside in the outward-facing (X_o) or inward-facing (X_i) conformation. For example, a physiological, ecf-to-cell Na^+ gradient increases the probability of finding the X_i confor-

mation of the antiporter. This effect of a substrate gradient on antiporter conformation is presumed to be the basis for *trans* acceleration of cation flow.

In our initial study of the antiporter we delineated three possible mechanisms for conductive Na^+ flow. These are indicated in Fig. 1 *B* (enclosed within the dashed boxes) as slip (*1*), electrodiffusion (*2*), and electrogenic stoichiometry (*3*). Slip (*1*) results from permitting the empty antiporter to recycle, that is, allowing the transition $X_i \rightleftarrows X_o$. Electrodiffusion (*2*) results from Na^+ flow through a channel-like conformation of the antiporter, $X_{'channel'}$. We chose to derive the conducting form of the antiporter from X_o, because this conformation is expected to be most abundant in the presence of an outward Na^+ gradient and least abundant in the presence of an inward Na^+ gradient. Electrogenic stoichiometry (*3*) refers to net charge translocation that results from a nonunity cation exchange ratio, shown in Fig. 1 *B* as the binding and translocation of more than one Na^+ ion per catalytic cycle.

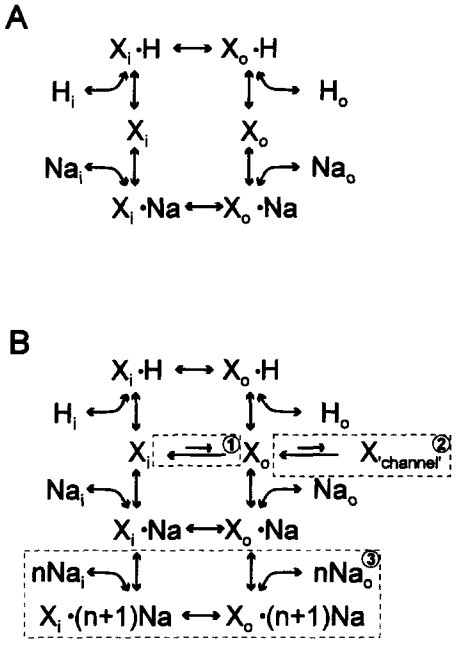

FIGURE 1. Stylized kinetic state diagrams of ping-pong kinetics for the Na-H antiporter. (*A*) Electroneutral operating modes of the Na-H antiporter. Subscript "i" refers to the inward- or cytosolic-facing conformation of the antiporter and subscript "o" refers to the outward- or extracellular fluid-facing conformation of the antiporter. See text for details. (*B*) Stylized kinetic model modified to include three possible mechanisms (shown within *dashed boxes*) for conductive Na^+ flow: (*1*) slip, (*2*) electrodiffusion, and (*3*) electrogenic stoichiometry.

The results presented here suggest that an electrogenic stoichiometry is sufficient to account for conductive Na^+ or Li^+ flow via the antiporter, although we were unable to rigorously exclude electrodiffusion as a mechanism for a portion of the outward Na^+ or Li^+ current. Slip, however, could be excluded as a mechanism of conductive Na^+ flow via the antiporter.

METHODS

Electrophysiology

Turtle colon (*Pseudemys scripta*), stripped of the serosal muscle layers, was mounted as a flat sheet in Ussing chambers (5.23 cm^2 in area) as previously described (Post and Dawson, 1992).

Transmural electrical potential difference was clamped to 0 mV (serosal bath as ground) and the resulting current (I_{SC}) was continuously monitored. Small signal conductance (G_T) was measured using a 10-mV, 1-s change in clamping potential. K Ringer's solutions was (in mM): 110 K, 2 Na, 1 Ca, 114 gluconate, 20 *N*-Tris(hydroxymethyl)methyl-3-aminopropanesulfonic (TAPS) acid, 10 dextrose (pH as indicated in text). In some experiments K^+ was replaced either by *N*-methyl-D-glucamine (NMDG), Li^+, or Cs^+, as indicated in the text. Na Ringer's solution was (in mM): 110 Na, 2 K, 1 Ca, 114 gluconate, 20 TAPS acid, 10 dextrose (pH as indicated in text). In some experiments TAPS acid was replaced by 2-(*N*-morpholino)ethanesulfonic (MES) acid or *N,N*-bis(2-hydroxyethyl)-2-aminoethanesulfonic (BES) acid. Baths were stirred by a gas lift system using room air. Inhibitors were added as a small volume of a concentrated stock solution (dimethylsulfoxide or H_2O was used as solvent). Amphotericin B was a gift of Squibb (Princeton, NJ), amiloride was a gift of Merck Sharp, & Dohme (Rahway, NJ), amiloride analogues were the gift of Dr. Tom Kleyman (Department of Medicine, University of Pennsylvania, Philadelphia, PA) or were purchased from Research Biochemicals Inc. (Natick, MA), $^{22}Na^+$ was purchased carrier free as NaCl from either New England Nuclear (Boston, MA) or Amersham Corp. (Arlington Heights, IL), and all other chemicals were purchased from either Fluka Chemical Corp. (Ronkonkoma, NY) or Sigma Chemical Co. (St. Louis, MO).

Current–Voltage Relation

Tissues, prepared as above, were mounted in perfusion chambers (0.5 cm^2 in area) and the transepithelial potential difference was clamped to 0 mV (serosal bath as ground) using an automatic voltage clamp with a sample-and-hold circuit. The data points for the current–voltage relation were obtained by adjusting the clamping potential to the indicated voltages for a 1-s duration and noting the current level at 200 ms after the onset of the voltage pulse. The mucosal perfusate was Na Ringer's solution and the serosal perfusate K Ringer's solution containing 100 μM ouabain. Both Ringer's solutions were at pH 6.5. Current–voltage relations were obtained after apical permeabilization with 10 μM amphotericin B and again after the addition of 1 mM amiloride to the serosal perfusate.

Identification of Na-H Antiport

Steep gradients of Na^+, Li^+, H^+, K^+, or Cs^+ were imposed across the basolateral membrane of osmotically shrunken colon and mucosal-to-serosal (MS) and serosal-to-mucosal (SM) $^{22}Na^+$ rate coefficients (λ^{Na}_{MS} and λ^{Na}_{SM}) were determined. We have previously shown that under these conditions amiloride sensitive Na-Na or Na-H counterflow and amiloride-sensitive outward current are via the Na-H antiporter (Post and Dawson, 1992).

Isotopic Measurements

Transmural fluxes of $^{22}Na^+$ were determined according to the method of Dawson (1977) using a 1-ml sample-and-replace paradigm repeated at 10-min intervals within each experimental condition. The "hot side" bath contained ~1 μCi of $^{22}NaCl$. 1 μM mucosal amiloride or 500 nM phenamil (to block apical Na^+ channels), and 100 μM serosal ouabain (to block the basolateral Na,K-ATPase) were present in all experiments. Unidirectional $^{22}Na^+$ rate coefficients (λ^{Na}_{MS} or λ^{Na}_{SM}) were calculated by dividing the "cold side" change in counts (cpm/cm^2·h) by the "hot side" concentration of $^{22}Na^+$ (cpm/ml). Unidirectional fluxes (J_{MS} or J_{SM}) were calculated as the product of the unidirectional rate coefficient (cm/h) and the "hot side" bath Na^+ concentration (meq/liter). Bath Na^+ and K^+ concentrations were determined by flame photometry.

Kinetics

Sigmoidal activation kinetics for antiporter–mediated currents (see Figs. 4 and 5) were analyzed by assuming either a high degree of cooperativity (Hill analysis) or the absence of any cooperativity (modified Eadie-Hofstee analysis) (Halm and Dawson, 1983). Analyses were performed on I_{SC} traces obtained from at least five tissues. Data were fit to linear transforms of both equations by a least squares linear regression. Basolateral, amiloride-sensitive Na^+ fluxes (see Figs. 8–11) were measured in at least three tissues for each data point. The amiloride-sensitive fluxes were fit to the Michaelis-Menten equation using a least squares, nonlinear regression algorithm.

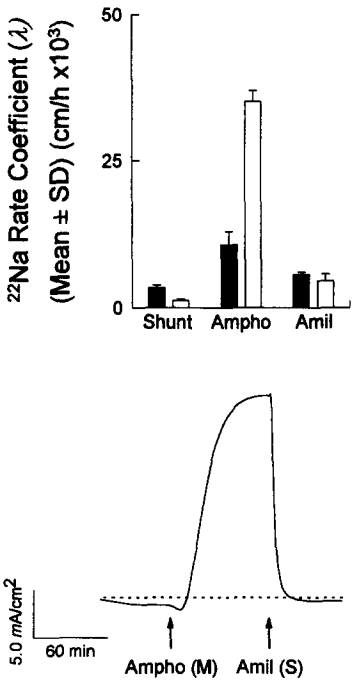

FIGURE 2. Unidirectional $^{22}Na^+$ rate coefficients (*top*) and outward Li^+ current (*bottom*) in the presence of an M-to-S Li^+ gradient. Mucosal bath contained Li Ringer's solution, pH 6.0 (MES), and 500 nM phenamil. Serosal bath contained K Ringer's solution, pH 6.0 (MES), and 100 μM ouabain. (*Top*) Before amphotericin permeabilization unidirectional rate coefficients for $^{22}Na^+$ flow, λ_{MS}^{Na} (■) and λ_{SM}^{Na} (□), were low. Apical permeabilization revealed an asymmetry in the rate coefficients, $\lambda_{SM}^{Na} > \lambda_{MS}^{Na}$, consistent with Li-$^{22}Na$ counterflow. Serosal 1 mM amiloride reduced the rate coefficients to near their pre-amphotericin levels. (*Bottom*) Apical permeabilization with mucosal amphotericin B (10 μM) revealed a Li^+-selective basolateral conductance, indicated by the increased M-to-S current flow (upward deflection of I_{SC}). Serosal amiloride (1 mM) reduced I_{SC} to near pre-amphotericin levels. (*Dotted line*) Zero current level.

RESULTS

Cation Selectivity and Inhibitor Specificity of the Basolateral Na-H Antiporter

In our previous study (Post and Dawson, 1992) we showed that an outwardly directed, M-to-S Na^+ gradient promoted $^{22}Na^+$ exchange and produced a Na^+-selective, amiloride-sensitive current. The data presented in Fig. 2 show that imposition of an M-to-S Li^+ gradient induced Li-^{22}Na counterflow and also an outward Li^+ current. Before the mucosal addition of amphotericin, transmural $^{22}Na^+$ flows were limited to the paracellular pathway and, accordingly, λ_{MS}^{Na} and λ_{SM}^{Na} were low and approximately

TABLE I

Activation of Na-H Antiporter-mediated Current and $^{22}Na^+$ Counterflow by Outward Na^+ or Li^+ Gradients

	λ_{SM}^{Na}	J_{SM}^{Na}	I_{SC}
	cm/h × 10³	*μEq/cm²h*	*μA/cm²*
M-to-S Na^+ gradient*	66.85§	0.23‖	7.98¶
	(7.25)	(0.024)	(4.64)
M-to-S Li^+ gradient‡	33.47§	0.11‖	14.44¶
	(10.25)	(0.036)	(6.02)

Values are the mean (SD), $n = 4$; values were obtained as the amiloride-sensitive portion of $^{22}Na^+$ flow or current flow in the presence of mucosal amphotericin B (10 μM) and serosal ouabain (100 μM).

*Mucosal bath contained 110 mM Na^+; serosal bath contained 2 mM Na^+ and no Li^+.

‡Mucosal bath contained 110 mM Li^+ and was nominally Na^+-free; serosal bath contained 2 mM Na^+ and no Li^+.

§$P < 0.005$ (t test).

‖$P < 0.005$ (t test).

¶Not statistically different at $P < 0.05$ (*t* test).

equal. Permeabilization of the apical membrane revealed a marked asymmetry in the transcellular $^{22}Na^+$ rate coefficients such that $\lambda_{SM}^{Na} > \lambda_{MS}^{Na}$, as expected for basolateral Li-Na counterflow. Serosal addition of 1 mM amiloride reduced the $^{22}Na^+$ rate coefficients to near their pre-amphotericin values. Initially (in the presence of 500 nM mucosal phenamil and 100 μM serosal ouabain) I_{SC} was near zero. Mucosal addition of amphotericin revealed a Li^+-selective conductance in the basolateral membrane, indicated by the large upward deflection of the I_{SC}. Serosal amiloride (1 mM) reduced I_{SC} to near zero. We compared, in paired tissues, the ability of similar gradients of Na^+ or Li^+ to drive *trans* acceleration of $^{22}Na^+$ flow via the antiporter and to generate antiporter-mediated short circuit currents. As shown in Table I the $^{22}Na^+$ counterflow associated with an M-to-S Li^+ gradient was significantly less than that associated with an M-to-S Na^+ gradient, while the outward currents in the two conditions were not statistically different. Gradients of Cs^+ or K^+ produced neither counterflow nor amiloride-sensitive current (data not shown). Thus, amiloride-

TABLE II

Comparison of the Inhibitor Sensitivities of the Exchange and Conductive Operating Models of the Basolateral Na-H Antiporter

Inhibitor	Current	Exchange
Organic agents		
Quinidine (2 mM)	100% Inhibition	100% Inhibition
Diphenylamine 2-carboxylate (1 mM)	100% Inhibition	100% Inhibition
Diethylpyrocarbonate (10 mM)	32% Inhibition	75% Inhibition
Inorganic cations		
Ni^+ (1 mM)	61% Inhibition	63% Inhibition
Co^{2+}	$K_i \sim 1.5$ mM	$K_i \sim 1.14$ mM
Gd^{3+}	$K_i \sim 6$ mM	$K_i \sim 7$ mM

Serosal addition of the following had no effect on either Na^+ exchange or current: 200 μM bumetanide, 100 μM verapamil, 500 μM nifedipine and 200 μM nicardipine, 10 mM Ba^{2+}, or 1 mM La^{3+}.

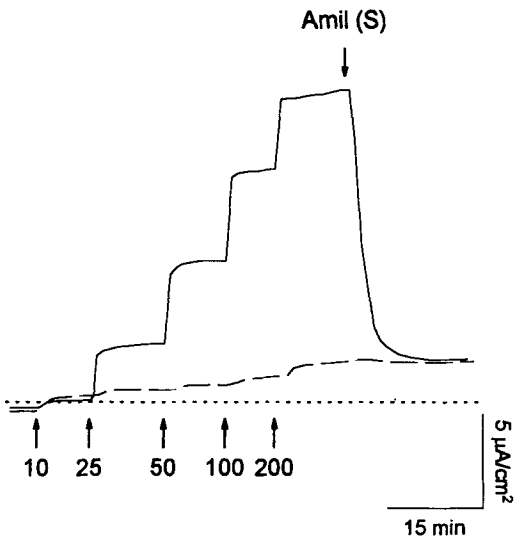

FIGURE 3. Stepwise increases in cytosolic Na^+ induced stepwise increases in I_{SC}. Mucosal bath contained K Ringer's solution, pH 6.5, and 1 μM amiloride; serosal bath contained K Ringer's solution and 100 μM ouabain. After amphotericin permeabilization (not shown) I_{SC} (*solid line*) was near zero. Mucosal Na^+ was increased by steps to (final concentrations): 10, 25, 50, 100, and 200 mM (*upward arrows*); I_{SC} increased with cation addition. Serosal amiloride (1 mM, *downward arrow*) reduced I_{SC} to near zero. Tissues preexposed to 1 mM serosal amiloride (*dashed line*) had attenuated I_{SC} changes in response to increases in mucosal Na^+. (*Dotted line*) Zero current level.

sensitive exchange and conduction were both selective for Na^+ and Li^+, but Na^+ was more effective at driving *trans* accelerated $^{22}Na^+$ flow.

Table II Serosal summarizes the effects of a variety of inhibitors on cation conduction and exchange, and demonstrates that inhibition of exchange activity was invariably accompanied by inhibition of conduction. The data in Fig. 2 and Table II

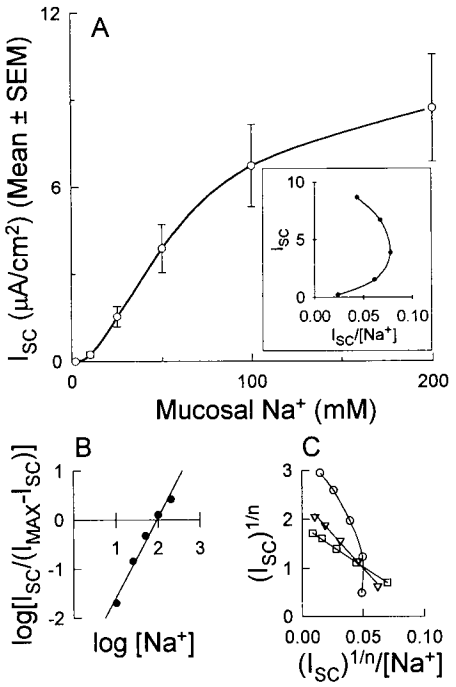

FIGURE 4. Kinetics of antiporter-mediated outward (M-to-S) Na^+ current. Mucosal and serosal baths were as in Fig. 3. (*A*) Antiporter-mediated Na^+ current displayed sigmoidal activation kinetics. Points are mean ± SEM, n = 7. (*Inset*): Eadie-Hofstee plot of the data. (*B*) Hill plot of data; Hill coefficient is 1.86 and K_{Na^+} is 75 mM. (*C*) Modified Eadie-Hofstee plot with I_{SC} raised to the $(1/n)$th power where n equals 2 (○), 3 (▽), or 4 (□); for n = 3 K_{Na^+} is 30 mM and for n = 4 K_{Na^+} is 20 mM.

are consistent with our previous conclusion (Post and Dawson, 1992) that the basolateral Na/H antiporter can mediate outward cation currents as well as cation exchange.

Na^+ and Li^+ Activation Kinetics of the Basolateral Conductance Are Sigmoidal

In the presence of mucosal amphotericin B (10 μM) and the absence of a Na^+ gradient, the I_{SC} was near zero, but stepwise addition of Na^+ (*upward arrows*) to the mucosal bath produced stepwise increases in I_{SC} (Fig. 3). addition of 1 mM amiloride (*downward arrow*) reduced I_{SC}, but not to the baseline value observed before the addition of mucosal Na^+. An identical experiment conducted in the presence of 1

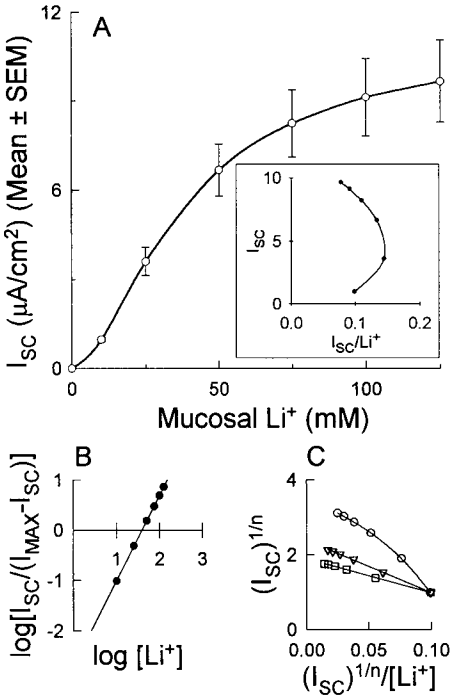

FIGURE 5. Kinetics of antiporter-mediated outward (M-to-S) Li^+ current. Mucosal and serosal baths were initially as in Fig. 3 except that aliquots of Li gluconate were employed to raise the mucosal Li^+ concentration. (*A*) Antiporter-mediated Li^+ current displayed sigmoidal activation kinetics. Points are mean ± SEM, n = 5. (*Inset*) Eadie-Hofstee plot of the data. (*B*) Hill plot of the data; Hill coefficient is 1.69 and K_{Li^+} is 38 mM. (*C*) Modified Eadie-Hofstee plot with I_{SC} raised to the $(1/n)$th power where n equals 2 (○), 3 (▽), or 4 (□); for n = 3 K_{Li^+} is 13 mM and for n = 4 K_{Li^+} is 9 mM.

mM serosal amiloride revealed an amiloride-insensitive, leakage current that was corrected for, when necessary, by linear extrapolation.

Activation by mucosal Na^+ of outward Na^+ current (Fig. 4 *A*) exhibited sigmoidal kinetics and could not be fit by the Michaelis-Menten equation. Fig. 4, *B* and *C*, illustrates two approaches to fitting the activation data (Halm and Dawson, 1983), a Hill plot (Fig. 4 *B*) and a modification of the Eadie-Hofstee plot (Fig. 4 *C*) that allows for multiple substrate binding in the absence of cooperativity. The Hill plot yielded a slope of 1.86 ± 0.16, consistent with an activation process requiring the highly cooperative binding of two Na^+ ions, and a K_{Na^+} of 75 ± 7 mM (mean ± SE). The Eadie-Hofstee plots were consistent with the independent binding of three to four Na^+ ions where the fit for the binding of three Na^+ ions yielded a K_{Na^+} of 30 ± 6 mM

and the fit for the binding of four Na^+ ions yielded a K_{Na^+} of 20 ± 5 mM (mean ± SE).[1] Activation by mucosal Li^+ of outward, amiloride-sensitive Li^+ current (Fig. 5 *A*) also exhibited sigmoidal kinetics. A Hill plot (Fig. 5 *B*) yielded a slope of 1.7 ± 0.06, consistent with the process of current activation requiring the highly cooperative binding of two Li^+ ions, and a K_{Li^+} of 38 ± 2 mM (mean ± SE). A modified Eadie-Hofstee plot (Fig. 5 *C*) yielded an estimate of three to four independent Li^+ binding events required for activation and K_{Li^+}'s of 13 ± 1 and 9 ± 2 mM (mean ± SE), respectively. The possible implications of these results will be considered in the Discussion.

Serosal Na^+ or Li^+ Inactivates Na Conductance

The observation that the amiloride sensitive basolateral Na^+ conductance was evoked by a cell-to-ecf Na^+ gradient, but was absent in the presence of either a

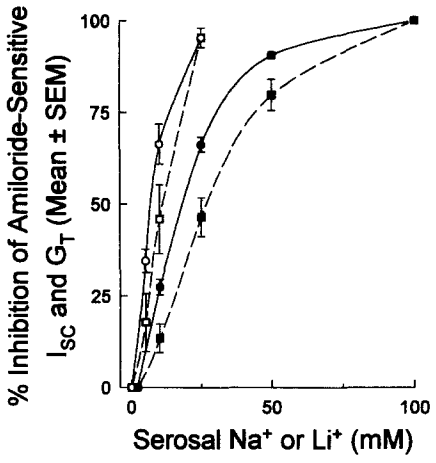

FIGURE 6. Dose–response curves for inhibition by serosal Na^+ or Li^+ of outward amiloride-sensitive Na^+ current (I_{SC}) and conductance (G_T). Mucosal bath contained Na Ringer's solution, pH 6.0 (MES), 500 nM phenamil, and 10 μM amphotericin B. Serosal bath contained K Ringer's solution, pH 6.0 (MES) and 100 μM ouabain. Aliquots of Na gluconate (●) or Li gluconate (○) to the serosal bath reduced I_{SC} in a dose-dependent manner. Aliquots of Na gluconate (■) or Li gluconate (□) to the serosal bath reduced G_T in a dose-dependent fashion. Points are mean ± SEM. $K_{1/2}$'s for inhibition of I_{SC} and G_T by Na^+ were 18 (n = 10) and 27 (n = 7) mM, respectively. $K_{1/2}$'s for inhibition of I_{SC} and G_T by Li^+ were 7 (n = 6) and 11 (n = 4) mM, respectively.

"physiological," ecf-to-cell Na^+ gradient (Post and Dawson, 1992) or symmetric mucosal and serosal Na^+ concentrations (ranging from 2 to 110 mM) (data not shown), prompted us to test the effect of raising extracellular Na^+ or Li^+ on the basolateral, amiloride-sensitive Na^+ conductance. Fig. 6 compares the effect of progressive increases in serosal Na^+ or serosal Li^+ on the Na^+ current (I_{SC}) and the small signal conductance (G_T). Two features of this plot are noteworthy. First, the amiloride-sensitive G_T was inhibited by the serosal addition of either Na^+ or Li^+. Second, Li^+ was more effective than Na^+ at reducing both the amiloride-sensitive I_{SC} and the amiloride-sensitive G_T. In additional experiments raising both the mucosal and serosal Na^+ concentration by 40 mM Na^+ in the presence of a cell-to-ecf Na^+

[1] It is important to note that, unlike the K_{Na} estimated by the Hill plot, the K_{Na} estimated by the modified Eadie-Hofstee plot is not the $K_{1/2}$, rather, it is the Na^+ concentration at which the slope of the sigmoidal curve (i.e., the rate of current activation) is maximal.

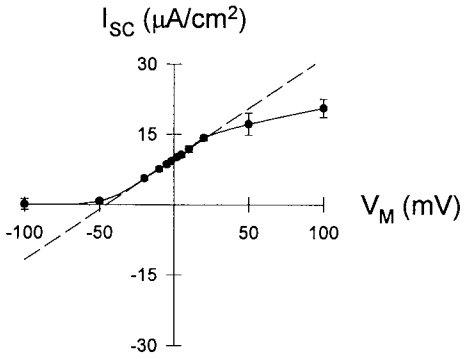

FIGURE 7. Current–voltage relation for the antiporter-mediated, outward Na^+ conductance. Mucosal bath contained Na Ringer's solution (110 mM Na^+, 2 mM K^+), pH 6.5, and 10 μM amphotericin B. Serosal bath contained K Ringer's solution (110 mM K^+, 2 mM Na^+), pH 6.5, and 100 μM ouabain. Current values were obtained at the indicated voltages in the absence and presence of 1 mM serosal amiloride; shown is the difference plot. *Dashed line:* linear regression on the ohmic portion of the current–voltage relation. Points are the mean ± SEM for five tissues.

gradient (i.e., maintaining ΔC_{Na^+} while increasing the serosal Na^+ concentration) decreased both the amiloride-sensitive I_{SC} and G_T (data not shown). Serosal addition of 50 mM NMDG gluconate (as an osmotic control) in the presence of a cell-to-ecf Na^+ gradient had no effect on the amiloride-sensitive outward Na^+ current (data not shown). Taken together these observations suggest that raising the extracellular concentration of Na^+ or Li^+ inactivates the basolateral Na^+ conductance.

The Current–Voltage Relation Is Not Compatible with Simple Diffusion

The current–voltage relation for the basolateral antiporter was determined by measuring currents in the presence of opposing cell-to-ecf (M-to-S) Na^+ and

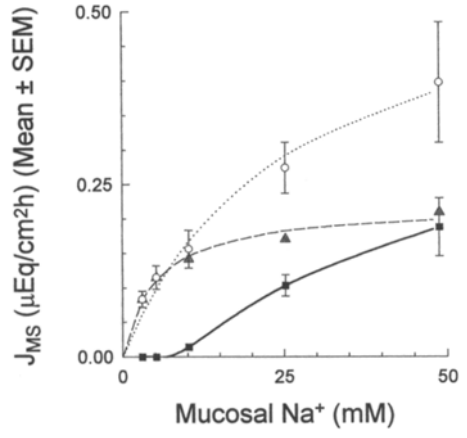

FIGURE 8. Activation kinetics of antiporter-mediated M-to-S (outward) Na^+ flux across the basolateral membrane at low *trans* (serosal) Na^+. Mucosal and serosal baths initially contained K Ringer's solution, pH 6.5; serosal bath contained 100 μM ouabain. After amphotericin permeabilization the mucosal Na^+ concentration was acutely increased from 2 mM to one of the indicated concentrations and the amiloride-sensitive portion of the M-to-S Na^+ flux determined. Only amiloride-sensitive fluxes are shown. As mucosal Na^+ increased the total Na^+ efflux (*dotted line*, ○) increased hyperbolically but the Na^+ current (*solid line*, ■) increased sigmoidally. The electroneutral portion of the total efflux (*dashed line*, △) was calculated as the difference between the total Na^+ efflux and Na^+ current plots. The apparent $K_{1/2}$ and J_{MAX} of the electroneutral efflux were 5.1 mM and 0.22 μeq/cm²h, respectively. Note that electroneutral Na exchange was nearly saturated at 10 mM Na^+ but outward Na^+ current was barely detectable.

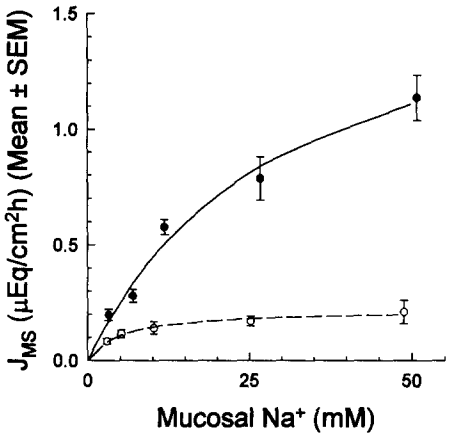

FIGURE 9. Activation kinetics of antiporter-mediated M-to-S (outward) Na^+ flux across the basolateral membrane at high *trans* (serosal) Na^+. Mucosal bath initially contained K Ringer's solution, pH 6.5, and serosal bath contained Na Ringer's solution, pH 6.5, and 100 μM ouabain. After amphotericin permeabilization the mucosal Na^+ concentration was acutely increased from 2 mM to one of the indicated concentrations, and the amiloride-sensitive portion of the M-to-S Na^+ flux (*solid line*, ●) determined. The apparent $K_{1/2}$ and J_{MAX} were 30 mM and 1.8 μeq/cm²·h, respectively. The electroneutral portion of the efflux at low *trans* Na^+ (*dashed line*, ○) from Fig. 8 is included for ease of comparison.

ecf-to-cell (S-to-M) K^+ gradients (pH 6.5), in the absence and then in the presence of serosal amiloride. Fig. 7 shows the difference plot, i.e., the current–voltage relation for the amiloride-sensitive pathway. The amiloride-sensitive current–voltage relation was ohmic around 0 mV but deviated from linearity beyond ~ ±25 mV. The reversal potential predicted from the slope of the ohmic portion of the plot was −45 mV, which yields a P_{Na^+}/P_{K^+} of ~6. However, the current never actually reversed as expected if K^+ was, in fact, impermeant. The shape of the current voltage relation is strikingly similar to that reported for the Na-glucose transporter (Parent, Supplisson, Loo, and Wright, 1992), although the Na-glucose cotransporter currents did not saturate until ±80 mV. However, the Na-H antiporter current–voltage relation is different from that reported for the Na-alanine transporter (Jauch, Peterson, and

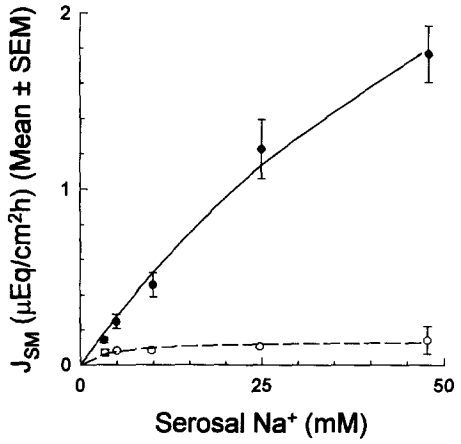

FIGURE 10. Activation kinetics of antiporter-mediated S-to-M (inward) Na^+ flux across the basolateral membrane at low (*dashed line*, ○) and at high (*solid line*, ●) *trans* (mucosal) Na^+ concentrations. Mucosal bath initially contained K Ringer's solution, pH 6.5 (low *trans*), or Na Ringer's solution, pH 6.5 (high *trans*), and serosal bath contained K Ringer's solution, pH 6.5, and 100 μM ouabain. After amphotericin permeabilization serosal Na^+ concentration was acutely increased from 2 mM to one of the indicated concentrations. Amiloride-sensitive portions of the flux are shown. The apparent $K_{1/2}$ increased from 4.3 to 76 mM Na^+, and the apparent J_{MAX} increased from 0.14 to 4.9 μeq/cm²·h as the *trans* Na^+ concentration was raised from 2 to 110 mM Na^+.

Laüger, 1986), where current was a linear function of voltage from −100 to +100 mV.

The current voltage relation shown in Fig. 7 was obtained with 2 mM Na^+ in the serosal bath. This raised the possibility that the lack of current reversal could also have resulted from the near absence of Na^+ ions in the serosal bath. To evaluate the effect of raising serosal Na^+, serosal Na^+ was increased to 20 mM to increase the availability of the charge carrier but minimize inhibition of the conductance. Once a stable I_{SC} had been established the tissues were clamped from 0 to 75 mV (mucosa negative). The serosal addition of 1 mM amiloride under these conditions had no effect on I_{SC} (data not shown). These results are consistent with the notion that the observed lack of current reversal in the current voltage relation was not due to a shortage of permeant ions in the serosal bath, but rather reflected an intrinsic, rectifying property of the conduction mechanism.

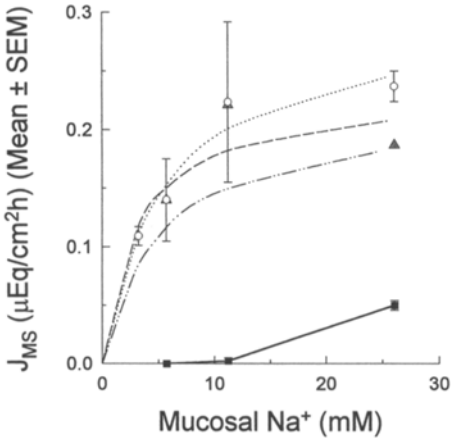

FIGURE 11. Activation kinetics of antiporter-mediated M-to-S (outward) Na^+ flux across the basolateral membrane at low *trans* (serosal) Na^+ at symmetric pH 8.5. Mucosal and serosal baths initially contained K Ringer's solution, pH 8.5 (TAPS); serosal bath also contained 100 μM ouabain. After amphotericin permeabilization the mucosal Na^+ concentration was acutely increased from 2 mM to one of the indicated concentrations. Only the amiloride-sensitive portions of the flux are shown in the plot. As mucosal Na^+ was increased the total Na^+ efflux (*dotted line*, ○) increased hyperbolically but the Na^+ current increased curvilinearly (*solid line*, ■). The electroneutral portion of the total efflux (*dashed line*, △) was calculated as the difference between the total Na^+ efflux and Na^+ current plots. The apparent $K_{1/2}$ of the electroneutral efflux was 3.2 mM Na^+; the apparent J_{MAX} was 0.23 μeq/cm²h. For comparison, the electroneutral Na^+ efflux (*dashed dotted line*) at symmetric pH 6.5 (Fig. 8) is also shown. Note that electroneutral Na exchange was nearly saturated at 10 mM Na^+ but that outward Na^+ current was barely detectable.

Kinetics of Antiporter-mediated Na^+ Influx and Efflux

Shown in Fig. 8 are the activation kinetics of the antiporter-mediated (i.e., amiloride-sensitive), total Na^+ efflux (M-to-S Na^+ flux), the conductive Na^+ efflux (amiloride-sensitive I_{SC}), and the calculated electroneutral Na^+ efflux (the difference between the total and conductive effluxes) at low *trans* (serosal) Na^+. The activation of Na^+ current by increased mucosal Na^+ displayed sigmoidal kinetics, consistent with the results presented in Fig. 4. The total Na^+ flux also increased, but in a manner more consistent with hyperbolic kinetics. The difference curve, which represents the electroneutral efflux of Na^+, is a hyperbolic function. Note that the electroneutral

flux was saturated at mucosal Na^+ values which were not sufficient to generate an appreciable current. An iterative fit of the difference curve to the Michaelis-Menten equation yielded an apparent $K_{1/2}$ for electroneutral efflux of 5.1 mM and a J_{MAX} of 0.22 μeq/cm²·h.

The ping-pong model (Fig. 1) predicts that raising the extracellular concentration of Na^+ will increase the relative abundance of the inward-facing forms of the antiporter, an effect that should be detectable as an increase in both the apparent $K_{1/2}$ and J_{MAX} for Na^+ efflux. The activation kinetics of Na^+ efflux in the presence of 110 mM serosal Na^+ are shown in Fig. 9. No correction for conductive flow was necessary as Na^+ current was absent in the presence of high extracellular Na^+ (see above). An iterative fit of the data to the Michaelis-Menten equation yielded an

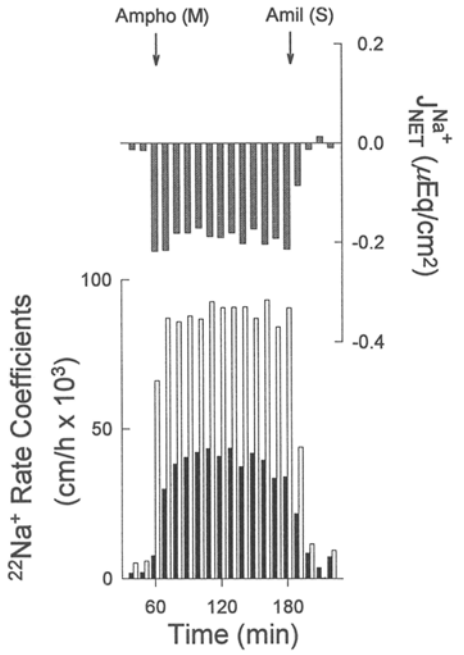

FIGURE 12. Unidirectional $^{22}Na^+$ rate coefficients and net transmural Na^+ flux in presence of an M-to-S proton gradient. Mucosal bath initially contained K Ringer's solution, pH 6.0 (MES), and 500 nM phenamil. Serosal bath contained K Ringer's solution, pH 8.5 (TAPS), and 100 μM ouabain. J_{NET} was calculated as $J^{Na}_{MS} - J^{Na}_{SM}$. Before apical permeabilization λ^{Na}_{MS} (■) and λ^{Na}_{SM} (□) were low and symmetric. Apical permeabilization (10 μM amphotericin B) revealed an asymmetry in the rate coefficients such that $\lambda^{Na}_{SM} > \lambda^{Na}_{MS}$, and a net S-to-M Na^+ flux. Serosal addition of 1 mM amiloride reduced both the unidirectional rate coefficients and the net flux to their pre-amphotericin levels.

apparent $K_{1/2}$ for Na^+ efflux (at high *trans* Na^+) of 30 mM and an apparent J_{MAX} of 1.8 μeq/cm²·h, six- and eight-fold greater, respectively, than the values obtained at low *trans* Na^+.

The activation kinetics for amiloride-sensitive, total Na^+ influx (i.e., S-to-M Na^+ flux) at low *trans* Na^+ (Fig. 1, *dashed line*) and at high *trans* Na^+ (Fig. 1, *solid line*) are shown in Fig. 10. No antiporter-mediated current flow was present in the low *trans* Na^+ condition. In the high *trans* Na^+ condition an antiporter mediated outward current was present, but was only appreciable at serosal Na^+ concentrations below 10 mM. The apparent $K_{1/2}$ for Na^+ influx at low *trans* Na^+ was 4.3 mM and the J_{MAX} was 0.14 μeq/cm²·h. Raising the *trans* Na^+ concentration increased the apparent $K_{1/2}$ for

Na^+ influx by 18-fold and the apparent J_{MAX} for Na^+ influx by 35-fold to 76 mM Na^+ and 4.9 μeq/cm²·h, respectively.

Na-Na Exchange Is Not Regulated by pH_i in Shrunken Cells

Na-Na exchange, like Na-H exchange, has been reported to be regulated by intracellular pH (Aronson, Nee, and Suhm, 1982). We tested for pH effects on Na-Na exchange in the permeabilized epithelium by comparing the activation of Na^+ efflux at pH 6.5 and at pH 8.5. Fig. 11 is a plot of the activation kinetics for Na^+ efflux (at low *trans* Na^+) at symmetric pH 8.5. For comparison, the activation kinetics for electroneutral Na^+ efflux at symmetric pH 6.5 (taken from Fig. 8) are also plotted. Over the Na^+ concentration range tested the curves for electroneutral efflux are virtually identical. Note that the maximal Na^+ concentration used was 25 mM; at pH

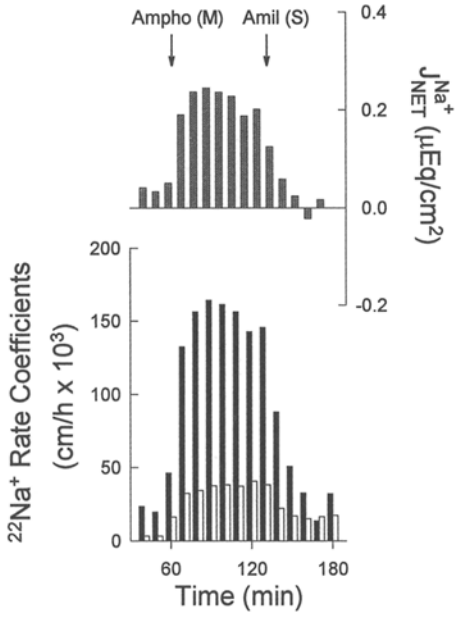

FIGURE 13. Unidirectional $^{22}Na^+$ rate coefficients and net transmural Na^+ flux in presence of an S-to-M proton gradient. Mucosal bath initially contained K Ringer's solution, pH 8.5 (TAPS), and 500 nM phenamil. Serosal bath contained K Ringer's solution, pH 6.0 (MES), and 100 μM ouabain. $J_{NET} > 0$ indicates net M-to-S Na^+ flux. Before apical permeabilization λ^{Na}_{MS} (■) and λ^{Na}_{SM} (□) were low and nearly symmetric. Apical permeabilization (10 μM amphotericin B) revealed an asymmetry in the rate coefficients, $\lambda^{Na}_{MS} > \lambda^{Na}_{SM}$, and a net M-to-S Na^+ flux. Serosal addition of 1 mM amiloride reduced both the unidirectional rate coefficients and the net flux to their pre-amphotericin levels.

8.5 large, amiloride-insensitive, leakage conductances precluded the determination of Na^+ efflux at cellular Na^+ concentrations exceeding 25 mM (not shown). Iterative fit of the electroneutral efflux to the Michaelis-Menten equation yielded a $K_{1/2}$ for Na^+ efflux of 3.16 mM and a J_{MAX} of 0.23 μeq/cm²·h.

Na-H Exchange Is Not Regulated by pH_i in Shrunken Cells

Na-H exchange activity has been reported to be decreased by an increase in the intracellular pH. This has been attributed to the existence of a "modifier site" for intracellular protons (Aronson et al., 1982). We tested for activation of Na-H exchange by cytosolic H^+ by comparing the ability of oppositely directed proton gradients to activate $^{22}Na^+$ exchange. In the absence of a proton gradient neither a net Na^+ flux nor *trans* acceleration of the tracer rate coefficients were discernable

(data not shown). In the presence of an M-to-S proton gradient (pH 6.0|pH 8.5; M|S), before amphotericin permeabilization, the rate coefficients were low and approximately equal and the net Na^+ flux (J_{NET}), calculated as $J^{Na}_{MS} - J^{Na}_{SM}$, was negligible (Fig. 12). The addition of 10 μM amphotericin B to the mucosal bath revealed that the rate coefficient for S-to-M $^{22}Na^+$ flow across the basolateral membrane was greater than that for M-to-S $^{22}Na^+$ flow. Amphotericin B permeabilization also revealed a net S-to-M flux of Na^+. Both the net Na^+ flux and the unidirectional rate coefficients were markedly reduced by serosal amiloride (1 mM). These results are consistent with the coupling of M-to-S proton flow to S-to-M Na^+ flow.

Reversing the direction of the pH gradient reversed the net Na^+ flux and the asymmetry in the unidirectional rate coefficients (Fig. 13). In the presence of an

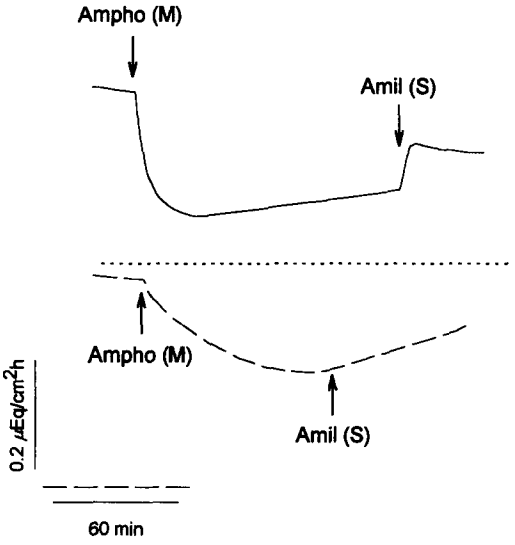

FIGURE 14. I_{SC} traces in the presence of M-to-S or S-to-M proton gradients. Traces were obtained from tissues represented in Fig. 12 (M-to-S proton gradient, *solid line*) and Fig. 13 (S-to-M proton gradient, *dashed line*). In the presence of an M-to-S H^+ gradient before amphotericin permeabilization the I_{SC} is consistent with M-to-S H^+ flow. Amphotericin permeabilization either inhibits this current or reveals an S-to-M current. Serosal amiloride (1 mM) restores the I_{SC} towards its pre-amphotericin levels, consistent with inhibition of S-to-M current flow across the basolateral membrane. The amiloride sensitive portion of the I_{SC} can be accounted for as a net Na^+ flux (compare with Fig. 12). In the presence of an S-to-M H^+ gradient I_{SC} was consistent with S-to-M H^+ flow; net Na^+ flux can not account for the I_{SC}. (*Dotted line*) Zero current level.

S-to-M proton gradient (pH 8.5|pH 6.0; M|S) and before mucosal amphotericin B addition, a small net M-to-S Na^+ flux was present. Amphotericin permeabilization of the apical membrane revealed a markedly increased net M-to-S Na^+ flux. The rate coefficient for M-to-S $^{22}Na^+$ flow across the basolateral membrane was greater than that for S-to-M $^{22}Na^+$ flow, consistent with Na-H counterflow. The serosal addition of 1 mM amiloride reduced the net flux to approximately zero. Note that in the face of proton gradients of identical magnitude the net Na^+ fluxes were approximately equal regardless of the direction of the proton gradient (compare Fig. 12, *top* and Fig. 13, *top*). The differences in the magnitudes of the *trans* accelerated rate coefficients resulted from small (~1 mM Na^+) differences in the bath Na^+ concentrations.

Proton Gradients Drive Anomalous Na^+ Currents

The scheme shown in Fig. 1 *B* for an electrogenic stoichiometry (box *3*) leads to the prediction that a H^+ gradient should drive an electrogenic counterflow of Na^+. In the face of, for example, an outward proton gradient, but in the absence of a Na^+ gradient, an amiloride-sensitive, inward Na^+ current should be present as a result of $(n + 1)Na^+:1H^+$ exchange. Fig. 14 shows the I_{SC} associated with the tissues in Figs. 12 and 13. In the presence of an M-to-S H^+ gradient an amiloride-sensitive, inward current was present; however, no amiloride-sensitive current was detected in the presence of an S-to-M proton gradient. In the presence of an M-to-S H^+ gradient the

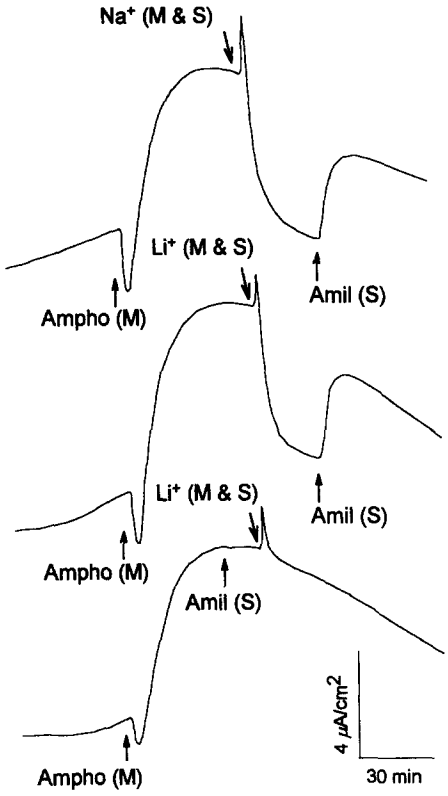

FIGURE 15. S-to-M current flow driven by an M-to-S proton gradient is activated by simultaneously raising mucosal and serosal Na^+ or Li^+ concentrations. Mucosal bath contained nominally Na^+ and Li^+ free, NMDG Ringer's solution, pH 6.0 (MES). Serosal bath contained nominally Na^+ and Li^+ free, NMDG Ringer's solution, pH 8.5 (TAPS), and 100 μM ouabain. The mucosal addition of amphotericin B revealed an M-to-S current that was unaffected by the serosal addition of 1 mM amiloride (*bottom trace*). Addition of 5 mM Na^+ (*top trace*) or 5 mM Li^+ (*middle trace*) to the mucosal and serosal baths resulted in a decrease in the current consistent with the development of an S-to-M current. Subsequent addition of 1 mM amiloride to the serosal bath allowed a partial recovery of the current.

net amiloride-sensitive Na^+ flux (0.1684 ± 0.024 μeq/cm²·h; mean ± SD) was more than sufficient to account for the amiloride-sensitive current (0.0954 ± 0.019 μeq/cm²·h; mean ± SD).

The cation selectivity of the inward current induced by an outward proton gradient was determined by exposing tissues to mucosal NMDG Ringer's solution, pH 6.0 and serosal NMDG Ringer's solution, pH 8.5; both solutions were Na^+ free. Amphotericin permeabilization revealed an M-to-S current (Fig. 15), presumably carried by protons, that was insensitive to serosal amiloride (1 mM) (*bottom trace*). Simultaneous addition to both the mucosal and serosal baths of either 5 mM Na^+ (*top trace*) or 5

mM Li^+ (*middle trace*) promptly decreased I_{SC}. The reduction could represent the inhibition of an M-to-S current or the activation of an S-to-M current. Consistent with the latter possibility, the serosal addition of amiloride (1 mM) increased the I_{SC}, and pretreatment of the tissues with serosal amiloride (1 mM) abolished the cation-induced change in I_{SC}. In similar experiments the addition of 5 mM K^+, Rb^+, or Cs^+ to the serosal and mucosal baths did not induce an amiloride-sensitive S-to-M current (not shown). These results are consistent with the notion that the proton-driven, counterflow current is selective for Na^+ and Li^+.

The proton-driven, counterflow current was completely inhibited by 20 μM EIPA, 5 μM DMA, or 1 mM amiloride. The $K_{1/2}$ for amiloride inhibition (at a serosal bath pH of 8.5) was ~30 μM, consistent with the sensitivity of a Na-H antiporter-mediated process, indicating that the Na-H antiporter can couple outward proton flow to inward, electrogenic Na^+ flow.

DISCUSSION

Na^+ Conduction Results from Electrogenic Na/Na or Na/H Exchange

We reported previously (Post and Dawson, 1992) that the basolateral Na-H antiporter is not restricted to electroneutral exchange, but can also function in a conductive operating mode. We suggested three possible conductive mechanisms: slip, electrodiffusion, and electrogenic stoichiometry. The results presented here suggest that an electrogenic stoichiometry can account for Na-H antiporter-mediated conduction; however, we cannot exclude the possibility that electrodiffusion mediates a portion of the outward current. Slip, however, can be excluded as a mechanism for Na-H antiporter-mediated conduction.

The observation that an outward (M-to-S) proton gradient could drive inward current was important for several reasons. First, the cation selectivity, the inhibitor sensitivity, and the activation of the current by an outward proton gradient suggested that the Na/H antiporter was mediating the current. Second, because the inward current was dependent on an outward proton gradient and was present in the absence of Na^+ or Li^+ gradients, this current met the most stringent test for an antiporter-mediated counterflow process: net flow of Na^+ (or Li^+) driven by an oppositely directed proton gradient. Third, the fact that this counterflow was, in part, electrogenic is strong evidence that under these conditions the antiporter can exhibit a nonunity exchange stoichiometry. In the context of a ping-pong kinetic model, conductive counterflow driven by an outward proton gradient can be accounted for by allowing the outward-facing conformation of the antiporter to bind and translocate more than one Na^+ per transport cycle (Fig. 1 *B*, box *3*). The sigmoidal kinetics of outward Na^+ current activated by cytosolic Na^+ are also consistent with an electrogenic transport mechanism which involves the binding of more than one Na^+, but in this case by the inward-facing form of the antiporter.

The slip mechanism (Fig. 1 *B*, box *1*) is unlikely to contribute to the observed conductive flows for several reasons. First, and most important, recycling of the unloaded transporter cannot account for conductive counterflow because the outward flow of protons would not be coupled to the inward movement of Na^+. Second, a slip mechanism should give rise to proton currents as well as to Na^+ currents, but

amiloride-sensitive proton currents were never observed. Third, a simple version of the slip mechanism predicts that as Na^+ exchange becomes saturated conductive Na^+ flow should decrease as a result of the decreased time average probability of finding the empty or unoccupied conformation of the antiporter (Kaplan et al., 1983; Knauf et al., 1983). In fact, we observed the opposite. At mucosal Na^+ concentrations sufficient to saturate Na^+ exchange, conductive Na^+ flow increased as the mucosal Na^+ concentration was increased (Fig. 8). And fourth, the slip mechanism predicts that for similar gradients of two substrates, that substrate with the greater apparent affinity for the antiporter should drive a smaller conductive flow as a result of a decreased time average probability of finding the unoccupied conformation of the antiporter (Knauf et al., 1983). The turtle colon basolateral Na/H antiporter appears to possess a greater apparent affinity for Li^+ than for Na^+, as has been reported for Na-H antiporters in other tissues (Kinsella and Aronson, 1981; Ives, Yee, and Warmock, 1983; Mahnensmith and Aronson, 1985; Knickelbein, Aronson, and Dobbins, 1990). This difference in affinity is suggested by the observations that, in the face of similar gradients of Na^+ and Li^+, Na^+-driven $^{22}Na^+$ counterflow was twofold greater than Li^+-driven $^{22}Na^+$ counterflow; and that serosal Li^+ was more effective than serosal Na^+ at inhibiting conductive Na^+ flow. For similar gradients of Na^+ and Li^+, the slip mechanism predicts that the Na^+ current will be greater in magnitude than the Li^+ current. In fact, if anything the Li^+ current was slightly greater than the Na^+ current.

Charge movement via a channel-like mechanism (Fig. 1 *B*, box *2*) can not account for a counterflow current driven by an outward proton gradient. However, in the case of outward (M-to-S) Na^+ current a component of the charge flow via a channel-like conformation of the antiporter cannot be excluded. The absence of amiloride-sensitive, outward proton currents in the presence of an outward proton gradient and our inability to reverse the direction of outward Na^+ current by altering the clamping potential would seem to point to a non–channel-like mechanism of current flow. However, rectification of the Na^+ current could be attributed to gating effects on the channel, and the absence of proton currents could result from the channel being impermeable to protons. Thus we cannot rule out the possibility of channel-mediated conduction by the antiporter under some conditions.

Stoichiometry and Asymmetry of the Antiporter

The activation kinetics for outward Na^+ currents together with the relative size of the conductive and electroneutral Na^+ flows in different conditions provides the basis for some speculation regarding the number of Na^+ transported per conductive transport cycle. We explored two approaches to the analysis of the activation kinetics: multiple, independent ion binding (modified Eadie-Hofstee) and highly cooperative multiple-ion binding (Hill). The former suggested that the activation of conduction could be accounted for by the independent binding of three or four Na^+ ions, whereas the latter can be interpreted in terms of activation requiring the binding of two Na^+ ions, but in a highly cooperative manner.

In a previous study (Post and Dawson, 1992), we found that in the presence of a large outward Na^+ gradient the total Na^+ efflux could be divided into two components; a conductive component of ~ 0.58 $\mu eq/cm^2 \cdot h$ and an electrically neutral

component of ~0.22 μeq/cm²·h. Na-H exchange in this condition appears to be small or absent so that the electrically silent component of the Na^+ efflux can be interpreted as resulting from Na-Na exchange. Accordingly, the Na^+ influx under these conditions was ~0.22 μeq/cm²·h. The ratio of conductive Na^+ efflux to Na^+ influx is 2.6, consistent with an electrogenic transport event involving the binding of three Na^+ ions, as suggested by the Eadie-Hofstee interpretation of the activation kinetics. However, if the standard errors of the conductive and exchange fluxes are taken into account, the calculated ratio can range from a minimum of 2.1 to a maximum of 3.2, so that these values cannot be used to distinguish between the two models.

Both analyses also provide an estimate of the apparent K_{Na} for the binding of Na^+ during the conductive cycle of the antiporter. A strict interpretation of the apparent K_{Na}'s of 75 mM (Hill analysis) or 20 or 30 mM (modified Eadie-Hofstee analysis) suggests that regardless of the degree of cooperativity between the binding sites the conduction event represents Na^+ bound with an affinity that is considerably less than that which characterizes electroneutral exchange, where the K_{Na} is ~5 mM. One interpretation of this low apparent affinity is that multiple ion binding by the antiporter occurs at sites different from those involved in one-for-one exchange.

Relative magnitudes of conductive and nonconductive Na^+ fluxes were also obtained from experiments in which a steep outward proton gradient was imposed in the presence of symmetric low Na^+ (2–4 mM), but these turned out to be less informative with respect to the choice of an appropriate kinetic description. Referring to the model shown in Fig. 1 *B*, if the only Na^+ transport process was the translocation of n ions in exchange for 1 H^+ per transport cycle, then for an $n = 4$ we would predict that the ratio of conductive to electroneutral Na^+ fluxes would be ~3, as in the experiments involving an outward Na^+ gradient. The measured values, however, show that the neutral flux actually exceeds the conductive by about a factor of 2. This is not unexpected, however, because it seems likely that in this condition a substantial fraction of the Na^+ flux will occur by the "singly bound," Na-H, pathway and thus will contribute nothing to the conductive component. The ratio of the conductive to electroneutral flux is, therefore, much less informative because the relative contributions of Na-H exchange and $(Na)_n$-H exchange to the total flux are unknown. This interpretation is supported by the observation that in some experiments the counterflow current was transient in spite of the fact that Na-H exchange was still evident as amiloride sensitive net Na^+ flow.

Taken together these results suggest the model for electrogenic Na^+ efflux depicted in Fig. 1 *B*, box *3* (note that the pathways enclosed by boxes *1* and *2* are not a part of this model). We assume that the Na^+ and Li^+ binding sites involved in one-for-one exchange are independent of those that participate in the conduction process. Consider the condition $V_M = 0$ and, initially, low intra- and extracellular Na^+ concentrations. As the cytoplasmic Na^+ concentration is raised the Na^+ binding site involved in one-for-one exchange is occupied first and becomes saturated at 10–15 mM $[Na]_i$ (Fig. 8). At this point Na^+ binding to other, lower-affinity sites on the antiporter becomes significant and an outward Na^+ current is initiated. To maintain this current the outward-facing form of the antiporter must revert to the inward-facing form and initiate another cycle of outward charge translocation. In the

presence of a steep, outward Na^+ gradient the recycling of the antiporter is expected to occur in one of two ways. Unloading of all of the bound Na^+ (high-affinity plus low-affinity sites) would generate an unloaded, outward-facing antiporter conformation which could recycle by binding either one Na^+ or one proton. Alternatively, Na^+ could unload from the low affinity sites and the singly bound, outward-facing form of the antiporter could revert to the singly bound, inward-facing form. This sequence of events is compatible with the observation that large outward gradients of Na^+ and Li^+ give rise to similar outward currents, but that Li^+ gradients are associated with reduced $^{22}Na^+$ counterflow. Counterflow is a measure of the availability of the outward-facing, unloaded form of the antiporter. The higher affinity of Li^+ for the antiporter binding sites might be expected to decrease the availability of the unloaded, outward-facing form of the antiporter due to the direct recycling of the singly bound form. This would decrease the $^{22}Na^+$ counterflow but have no effect on the rate of outward charge translocation; that would be limited by the antiporter's rate of conformational cycling.

Inward Na^+ or Li^+ currents driven by an outward proton gradient can also be accounted for by this model. An outward proton gradient would be expected to lead to a redistribution of antiporter conformations which favors outward-facing forms. This would allow occupancy of both the one-for-one exchange site and the multiple ion binding sites by extracellular Na^+ or Li^+. Thus, both Na-H exchange and inward currents can be accounted for by this model.

The simple model presented here (Fig. 1 *B*, box *3*) is symmetric; either inward or outward cation gradients should be able to drive current flow. This is clearly not the case. Amiloride-sensitive, conductive transport was not discernable when V_M was clamped to ±60 mV in the presence of symmetric mucosal/serosal Na^+ concentrations from 2:2 to 110:110 mM; nor was conductive transport observed in the presence of symmetric Na^+/Li^+ or Li^+/Na^+ concentrations. Furthermore, inward Na^+ or Li^+ gradients did not induce inward currents nor did an inward proton gradient induce an outward current. With reference to Fig. 1 *B*, box *3*, the simplest, unified interpretation of these results is that an outward gradient of Na^+, Li^+, or H^+ predisposes the antiporter toward multiple Na^+ or Li^+ binding by either the outward- or inward-facing form of the antiporter, and that multiple ion binding can be manifest as a current. Raising the serosal Na^+ or Li^+, but not proton, concentration inhibits multiple Na^+ or Li^+ binding.

Inactivation of outward currents by extracellular Na^+ or Li^+ could explain why Na/H antiporter mediated currents have not been previously reported. Reviews by Aronson (1985) and Montrose and Murer (1988) cite a number of observations of electroneutral or unity stoichiometry, but examination of these studies revealed that the experimental conditions generally employed (i.e., low cell and high ecf Na^+ concentrations) would not be expected to lead to conductive Na^+ flow.

We were not able to detect a regulatory effect of pH on Na-H or Na-Na exchange activity in shrunken cells. This is in contrast to some (Wakabayashi, Fafournoux, Sardet, and Pouysségur, 1992; Grinstein, Rothstein, and Cohen, 1985; Aronson et al., 1982) but not other (Knicklebein et al., 1990; Manganel and Turner, 1989) studies. It may be that activation by cell shrinking precludes further activation by cytosolic protons, or that the basolateral Na-H antiporter of colon lacks a proton activation

site. On the other hand, the observed effects of outward gradients in promoting cation conduction raises the possibility of some asymmetry in the antiporter that could have regulatory significance.

Is Antiporter-mediated Conduction Important?

In view of the ionic conditions required to evoke conductive Na^+ flow via the exchanger it seems unlikely that such a process would play a physiological role in the cell under normal conditions. In the presence of the inwardly directed Na^+ gradient that typifies vertebrate cells, antiporter-mediated transport events would be restricted to one-for-one exchange of Na^+, Li^+, and H^+. However, antiporter-mediated charge translocation could have important implications with regard to the mechanism of the catalytic cycle that underlies the ion translocation process. In this respect it is particularly important that conduction appears to occur by means of cation exchange rather than pore-mediated electrodiffusion, so that future studies of charge translocation might be expected to provide insight into the conformational changes that are the basis for cation exchange.

We would like to thank Dr. Tom Kleyman for the generous gifts of ethlyisopropylamiloride, dimethylamiloride, and phenamil; Merck Sharp & Dohme for their gift of amiloride; and Squibb for their gift of amphotericin B. Nancy Kushman and John Dickason provided invaluable technical assistance.

This research was supported by grants from the National Institute of Diabetes and Digestive and Kidney Diseases (DK-29786), the University of Michigan Gastrointestinal Peptide Center (DK-34933), and the American Heart Association of Michigan (901G34).

Original version received 24 May 1993 and accepted version received 7 December 1993.

REFERENCES

Aronson, P. 1985. Kinetic properties of the plasma membrane Na-H exchanger. *Annual Review of Physiology.* 47:545–560.

Aronson, P. S., J. Nee, and M. A. Suhm. 1982. Modifier role of internal H^+ in activating the Na-H exchanger in renal microvillus membrane vesicles. *Nature.* 299:161–163.

Dawson, D. C. 1977. Na and Cl transport across the isolated turtle colon: parallel pathways for transmural ion movement. *Journal of Membrane Biology.* 37:213–233.

De Weer, P., and R. Rakowski. 1984. Current generated by backward-running electrogenic Na pump in squid giant axons. *Nature.* 309:450–452.

Fröhlich, O., and R. B. Gunn. 1986. Erythrocyte anion transport: the kinetics of a single-site obligatory exchange system. *Biochimica et Biophysica Acta.* 864:169–194.

Gadsby, D. C., M. Nakao, A. Bahinski, G. Nagel, and M. Suenson. 1992. Charge movements via the cardiac Na,K-ATPase. *Acta Physiologica Scandinavica Supplementum.* 607:111–123.

Grinstein, S., A. Rothstein, and S. Cohen. 1985. Mechanism of osmotic activation of Na^+/H^+ exchange in rat thymic lymphocytes. *Journal of General Physiology.* 85:765–787.

Halm, D. R., and D. C. Dawson. 1983. Cation activation of the basolateral sodium-potassium pump in turtle colon. *Journal of General Physiology.* 82:315–329.

Hunter, M. J. 1977. Human erythrocyte anion permeabilities measured under conditions of net charge transfer. *Journal of Physiology.* 268:35–49.

Ives, H. E., V. J. Yee, and D. G. Warnock. 1983. Mixed type inhibition of the renal Na-H antiporter by Li^+ and amiloride. *Journal of Biological Chemistry.* 258:9710–9716.

Jauch, P., O. H. Peterson, and P. Läuger. 1986. Electrogenic properties of the sodium-alanine cotransporter in pancreatic acinar cells. I. Tight-seal whole-cell recordings. *Journal of Membrane Biology.* 94:99–115.

Kaplan, J. H., P. B. Dunham, P. J. Logue, and L. J. Kenney. 1984. Na/Na exchange through the Na/K pump of HK sheep erythrocytes. *Journal of General Physiology.* 84:839–844.

Kaplan, J. H., M. Pring, and H. Passow. 1983. Band-3 protein-mediated anion conductance of the red cell membrane: slippage vs ionic conductance. *FEBS Letters.* 156:175–179.

Kinsella, J. L., and P. S. Aronson. 1981. Interaction of NH_4^+ and Li^+ with the renal microvillus membrane Na^+-H^+ exchanger. *American Journal of Physiology.* 241:C220–C226.

Knauf, P. A., F.-Y. Law, P. J. Marchant. 1983. Relationship of net chloride flow across the human erythrocyte membrane to the anion exchange mechanism. *Journal of General Physiology.* 81:95–126.

Knickelbein, R. G., P. S. Aronson, and J. W. Dobbins. 1990. Characterization of Na-H exchangers on villus cells in rabbit ileum. *American Journal of Physiology.* 259:G802–G806.

Mahnensmith, R. L., and P. S. Aronson. 1985. Interrelationships among quinidine, amiloride, and lithium as inhibitors of the renal Na^+-H^+ exchanger. *Journal of Biological Chemistry.* 260:12586–12592.

Manganel, M., and J. Turner. 1989. Agonist induced activation of Na-H exchange in rat parotid acinar cells. *Journal of Membrane Biology.* 111:191–198.

Montrose, M. H., and H. Murer. 1988. Kinetics of Na-H exchange. *In* Na^+-H^+ Exchange. S. Grinstein, editor. CRC Press, Boca Raton, FL. 57–75.

Parent, L., S. Supplisson, D. D. Loo, and E. M. Wright. 1992. Electrogenic properties of the cloned Na-glucose cotransporter. I. Voltage-clamp studies. *Journal of Membrane Biology.* 125:49–62.

Post, M. A., and D. C. Dawson. 1992. Basolateral Na-H antiporter: uncoupled Na transport produces an amiloride-sensitive conductance. *American Journal of Physiology.* 262:C1089–C1094.

Stein, W. D. 1986. Intrinsic, apparent, and effective affinities of co- and countertransport systems. *American Journal of Physiology.* 250:C523–C533.

Wakabayashi, S., P. Fafournoux, C. Sardet, and J. Pouysségur. 1992. The Na-H antiporter cytoplasmic domain mediates growth factor signals and controls "H-sensing." *Proceedings of the National Academy of Sciences.* 89:2424–2428.